Boron Dipyrromethene (Bodipy) Phosphorescence Revealed in [Ir(ppy)(2)(bpy-CC-Bodipy)](+)

ARTICLE *in* INORGANIC CHEMISTRY · MARCH 2010

Impact Factor: 4.76 · DOI: 10.1021/ic901996u · Source: PubMed

5 AUTHORS, INCLUDING:

Aaron Rachford
Dow Chemical Company
29 PUBLICATIONS **803** CITATIONS
SEE PROFILE

Thomas Bura
French National Centre for Scientific Research
28 PUBLICATIONS **1,045** CITATIONS
SEE PROFILE

3730 *Inorg. Chem.* **2010**, *49*, 3730–3736
DOI: 10.1021/ic901996u

Inorganic Chemistry
Article

Boron Dipyrromethene (Bodipy) Phosphorescence Revealed in $[Ir(ppy)_2(bpy\text{-}C{\equiv}C\text{-}Bodipy)]^+$

Aaron A. Rachford,[†,∥] Raymond Ziessel,*[,‡] Thomas Bura,[‡] Pascal Retailleau,[§] and Felix N. Castellano*[,†]

[†]*Department of Chemistry and Center for Photochemical Sciences, Bowling Green State University, Bowling Green, Ohio 43403,* [‡]*Laboratoire de Chimie Organique et Spectroscopie Avancées, associé au Centre National de la Recherche Scientifique (LCOSA-CNRS), Ecole de Chimie, polymères, Matériaux (ECPM), 25 rue Becquerel 67087 Strasbourg Cedex, France, and* [§]*Laboratoire de Crystallochimie, ICSN - CNRS, Bât 27 - 1 avenue de la Terrasse, 91198 Gif-sur-Yvette, Cedex, France.* [∥]*Current address: The Dow Chemical Company, Analytical Sciences, 1897 Building, Midland, Michigan 48667.*

Received October 8, 2009

The synthesis, structural characterization, electrochemistry, and molecular photophysics of $[Ir(ppy)_2(bpy\text{-}C{\equiv}C\text{-}Bodipy)](PF_6)$, where ppy is 2-phenylpyridine and bpy-C≡C-Bodipy is 5-ethynyl-2,2′-bipyridine-8-phenyl-1,3,5,7-tetramethyl-4,4-bis(2,5-dioxaoct-7-ynyl)-4-bora-3*a*,4*a*-diaza-s-indacene (**4**), is presented. Static and dynamic photoluminescence and absorption measurements in conjunction with cyclic voltammetry were employed to elucidate the nature of the intramolecular energy transfer processes occurring in the excited state of the title chromophore. Parallel studies were performed on appropriate model chromophores (**2** and **3**) intended to represent the photophysics of the isolated molecular subunits, that is, triplet metal-to-ligand-charge-transfer (^{3}MLCT) and triplet Bodipy intraligand (^{3}IL) excited states, respectively. Upon charge transfer excitation of the title chromophore, the ^{3}MLCT based phosphorescence readily observed in **2** (Φ_{em} = 0.027, τ = 243 ns) is quantitatively quenched resulting from production of the ^{3}Bodipy excited state through intramolecular triplet−triplet energy transfer. The formation of the ^{3}Bodipy-localized excited state is confirmed by features in the transient absorption difference spectrum, extended excited-state lifetime (τ = 25 μs), as well the observation of ^{3}IL Bodipy-based phosphorescence detected at 730 nm at 77 K. The low temperature Bodipy phosphorescence is readily produced in **4** as a result of the internal Ir(III) heavy atom.

Introduction

Polychromophoric molecules comprising covalently linked organic or transition metal subunits dedicated to photoinduced energy transfer have attracted much attention as models for solar energy conversion processeses.[1,2] Taking advantage of the tunable photophysical properties of Ru(II), Os(II), Re(I), and Pt(II) residues, these luminescent complexes have often been involved in energy/electron transfer from their triplet metal-to-ligand-charge-transfer excited states (^{3}MLCT).[3] Along these lines supramolecular Ru/Pt[4] or Ru/Pd[5,6] complexes have been shown to produce charge separation promoting both formation of hydrogen and nanosized noble metal particles and colloids.[6] In terms of light harvesting, a variety of smart hybrid systems (organic/transition metals) have been purposely engineered using light-absorbing organic dyes for energy "input" and metalloporphyrins as light-emissive acceptors for energy "output".[7] We have also employed MLCT excited states for light-harvesting applications.[8] In recent examples related to the

*To whom correspondence should be addressed. E-mail: castell@bgsu.edu (F.N.C.), ziessel@unistra.fr (R.Z.).

(1) Balzani, V.; Credi, A.; Venturi, M. *Molecular Devices and Machines: Concepts and Perspectives for the Nanoworld*, 2nd ed.; Wiley-VCH: Weinheim, 2008.
(2) (a) Serin, J. M.; Brousmiche, D. W.; Fréchet, J. M. J. *Chem. Commun.* **2002**, 2605–2607. (b) Weil, T.; Reuther, E.; Mullen, K. *Angew. Chem., Int. Ed.* **2002**, *41*, 1900–1904. (c) Cotlet, M.; Vosch, T.; Habichi, S.; Weil, T.; Mullen, K.; Hofkens, J.; De Schryver, F. *J. Am. Chem. Soc.* **2005**, *127*, 9760–9768.
(3) *Top. Curr. Chem.* **2007**, *281*, entire volume.
(4) (a) Ozawa, H.; Haga, M.; Sakai, K. *J. Am. Chem. Soc.* **2006**, *128*, 4926–4927. (b) Ozawa, H.; Yokoyama, Y.; Haga, M.; Sakai, K. *Dalton Trans.* **2007**, 1197–1206.
(5) Rau, S.; Schäfer, B.; Gleich, D.; Anders, E.; Rudolph, M.; Friedrich, M.; Görls, H.; Henry, W.; Vos, J. G. *Angew. Chem., Int. Ed.* **2006**, *45*, 6215–6218.
(6) Lei, P.; Hedlund, M.; Lomoth, R.; Rensmo, H.; Johansson, O.; Hammarström, L. *J. Am. Chem. Soc.* **2008**, *130*, 26–27.
(7) Holten, D.; Bocian, D. F.; Lindsey, J. S. *Acc. Chem. Res.* **2002**, *35*, 57–69.
(8) (a) Tyson, D. S.; Luman, C. R.; Castellano, F. N. *Inorg. Chem.* **2002**, *41*, 3578–3586. (b) Tyson, D. S.; Henbest, K. B.; Bialecki, J.; Castellano, F. N. *J. Phys. Chem. A* **2001**, *105*, 8154–8161. (c) Tyson, D. S.; Luman, C. R.; Zhou, X.; Castellano, F. N. *Inorg. Chem.* **2001**, *40*, 4063–4071. (d) Tyson, D. S.; Castellano, F. N. *J. Phys. Chem. A.* **1999**, *103*, 10955–10960. (e) Tyson, D. S.; Castellano, F. N. *Inorg. Chem.* **1999**, *38*, 4382–4383. (f) Zhou, X.; Tyson, D. S.; Castellano, F. N. *Angew. Chem., Int. Ed.* **2000**, *39*, 4301–4305. *Angew. Chem.* **2000**, *112*, 4471−4475. (g) Lee, S. J.; Luman, C. R.; Castellano, F. N.; Lin, W. *Chem. Commun.* **2003**, 2124–2125. (h) Goze, C.; Kozlov, D. V.; Tyson, D. S.; Ziessel, R.; Castellano, F. N. *New J. Chem.* **2003**, *27*, 1679–1683. (i) Kozlov, D. V.; Tyson, D. S.; Goze, C.; Ziessel, R.; Castellano, F. N. *Inorg. Chem.* **2004**, *43*, 6083–6092.

 Published on Web 03/19/2010

current contribution, a single boron dipyrromethene (Bodipy) entity (singlet emitter at 540 nm) has been successfully tethered to Ru-terpyridine,[9] Ru-bipyridine,[10] Zn-terpyridine,[11] and Pt-terpyridine[12] producing more complex metal-organic multichromophoric structures. We note that we have recently exploited the triplet excited states in two distinct Bodipy chromophores in low power upconversion schemes based on sensitized triplet−triplet annihilation.[13]

Neutral and ionic iridium(III) complexes also display rewarding spectroscopic properties[14] and have found interesting applications in light emitting diodes,[15] oxygen sensors,[16] biological labeling reagents,[17] luminescent biological probes,[18] and protein staining.[19] The long-lived emitting states ($\tau > 300$ ns) and high room temperature (RT) photoluminescence quantum efficiencies ($\Phi_{PL} \sim 1$ for $[Ir(ppy)_3]$)[20] prompted us to link orthometalated Ir(III) complexes to boron dipyrromethene (Bodipy) fluorophores to promote (i) intersystem crossing between the singlet and triplet excited states of the linked Bodipy dyes due to strong spin−orbit coupling provided by the iridium center, and (ii) energy transfer between the metal center and the Bodipy subunits.

One difficulty with Ir(III) complexes relates to controlling the stereochemistry when polypyridyl ligands are chelated to the metal.[21] Many possible type of ligation are found with classical bipyridine or terpyridine ligands in particular N^N chelation versus N^C chelation.[22] To avoid these synthetic complications we decided to use a well-defined orthometalated dimer which is a rather versatile starting material to introduce ligands carrying a reactive functionality (an alkyne in our case). No significant experimental chemistry effort has been expended using iridium(III) complexes as metallo-synthons to graft additional functional modules such as an organic chromophore.[23] Herein we present the synthesis and characterization of an iridium(III) chromophore tethered to a Bodipy moiety. The photophysical properties have been investigated and compared to that of model chromophores which adequately describe the two subunits within the title compound. Using an ensemble of techniques including cyclic voltammetry as well as static and dynamic absorption and emission spectroscopy we demonstrate that selective excitation of the Ir(III) subunit is followed by efficient triplet−triplet energy transfer, ultimately sensitizing the long-lived ^{3}Bodipy ligand-localized excited state.

Experimental Section

General Procedures. All reactions were performed under a dry atmosphere of argon using standard Schlenk tube techniques. All chemicals were used as received from commercial sources without further purification unless otherwise stated. CH_2Cl_2 and CH_3CN were distilled from P_2O_5 under an argon atmosphere. NEt_3 was allowed to stand over KOH pellets prior to use. Benzene was used as received. ^{1}H NMR (300.1 MHz) and ^{13}C NMR (75.5 MHz) spectra were recorded at RT on a Bruker Avance 300 MHz spectrometer using perdeuterated solvents as internal standards (δ $CDCl_3$ 7.26 ppm). Chromatographic purifications were performed using deactivated alumina (including 6% water by weight). TLC was performed on silica gel or alumina plates coated with fluorescent indicator. Mass spectra were measured with a JEOL JMS-T100 LO Acc TOF (ESI-MS). Elemental analysis was conducted by an Elementar vario MICRO Cube.

Reagents. All reagents were used directly as obtained commercially unless otherwise noted. $[Ir(C^N)_2Cl]_2$ complex **1**,[21] 5-ethynyl-2,2′-bipyridine,[24] and 8-(4-iodophenyl)-1,3,5,7-tetramethyl-4,4-bis(2,5-dioxaoct-7-ynyl)-4-bora-3*a*,4*a*-diaza-s-indacene dye **3**,[25] were prepared according to literature protocols.

Complex 1. ^{1}H NMR (300.1 MHz, $CDCl_3$): δ 9.24 (d, ^3J = 5.8 Hz, 2H), 7.87 (d, ^3J = 8.1 Hz, 2H), 7.73 (td, ^3J = 7.2 Hz, ^4J = 1.3 Hz, 2H), 7.48 (d, ^3J = 7.2 Hz, 2H), 6.68 (q, ^3J = 7.2 Hz, ^4J = 1.3 Hz, 4H), 6.56 (td, ^3J = 7.5 Hz, ^4J = 1.2 Hz, 2H), 5.93 (d, ^3J = 7.2 Hz, 2H).

Complex 2. The dimeric complex **1** (0.102 g, 0.095 mmol) was dissolved in dichloromethane (6 mL) and methanol (6 mL), and 5-ethynyl-2,2′-bipyridine[24] (0.042 g, 0.233 mmol) was added as a solid. The mixture was heated at 60 °C during the night. The color of the solution turned progressively from orange to red. The solution was cooled down to RT, and the solvent evaporated to dryness. The residue was dissolved in DMF (1 mL) and dropwise added through a pad of Celite into an aqueous solution of KPF_6 (0.500 g in 20 mL water). The precipitate was collected on paper and washed with water (3 times 100 mL). The complex was dried in air and was purified by column chromatography on alumina. The desired complex (yellow band) was eluted with a gradient of methanol (0−1%) in dichloromethane as mobile phase. The analytically pure complex was obtained as orange crystals by crystallization in a mixture acetonitrile/diethylether (0.130 g, 83%). ^{1}H NMR (300.1 MHz, $CDCl_3$): δ 8.65 (d, ^3J = 8.5 Hz, 2H), 8.16 (d, ^3J = 7.7 Hz, 2H), 7.94 (m, 4H), 7.78 (td, ^3J = 7.7 Hz, ^4J = 1.7 Hz, 2H), 7.68 (d, ^3J = 7.2 Hz, 1H), 7.62 (d, ^3J = 7.2 Hz, 1H), 7.49 (t, ^3J = 6.6 Hz, 2H), 7.41 (t, ^3J = 6.6 Hz, 1H), 7.04 (q, ^3J = 7.8 Hz, ^4J = 1.3 Hz, 4H), 6.91 (m, 2H), 6.27 (t, ^3J = 6.6 Hz, 2H), 3.34 (s, 1H). ^{13}C{^{1}H} NMR (75.47 MHz, $CDCl_3$) δ 167.7, 167.6, 155.2, 155.0, 152.6, 150.3, 149.5, 148.64, 148.60, 143.4, 143.5, 142.6, 139.9, 138.3, 138.2, 131.7, 131.6, 130.93, 130.88, 128.4, 125.9, 124.9, 124.8, 123.6, 123.53, 123.47, 122.87, 122.78, 119.75, 119.7, 85.4, 78.1 ppm. ESI-MS (positive mode in CH_3CN) m/z 681.2 $([M - PF_6]^+$. Anal. Calcd for $C_{34}H_{24}N_4IrPF_6$ (M_r = 825.76): C, 49.45; H, 2.93; N, 6.78. Found C, 49.23, H, 2.78, N, 6.52.

(9) Galletta, M.; Campagna, S.; Quesada, M.; Ulrich, G.; Ziessel, R. *Chem. Commun.* **2005**, 4222–4224.
(10) Galletta, M.; Puntoriero, F.; Campagna, S.; Chiorboli, C.; Quesada, M.; Goeb, S.; Ziessel, R. *J. Phys. Chem. A* **2006**, *110*, 4348–4358.
(11) Harriman, A.; Rostron, J. P.; Cesario, M.; Ulrich, G.; Ziessel, R. *J. Phys. Chem. A* **2006**, *110*, 7994–8002.
(12) Nastasi, F.; Puntoriero, F.; Campagna, S.; Diring, S.; Ziessel, R. *Phys. Chem. Chem. Phys.* **2008**, *10*, 3982–3986.
(13) Singh-Rachford, T. N.; Haefele, A.; Ziessel, R.; Castellano, F. N. *J. Am. Chem. Soc.* **2008**, *130*, 16164–16165.
(14) Lowry, M. S.; Bernhard, S. *Chem.—Eur. J.* **2006**, *12*, 7970–7977.
(15) Adachi, C.; Baldo, M. A.; Forrest, S. R.; Lamansky, S.; Thompson, M. E.; Kwong, R. C. *Appl. Phys. Lett.* **2001**, *78*, 1622–1624 and references therein.
(16) DiMarco, G.; Lanza, M.; Pieruccini, M.; Campagna, S. *Adv. Mater.* **1996**, *8*, 576–580.
(17) Lo, K. K. W.; Hui, W. K.; Chung, C. K.; Tsang, K. H. K.; Lee, T. K. M.; Li, C. K.; Lau, J. S. Y.; Ng, D. C.-M. *Coord. Chem. Rev.* **2006**, *250*, 1724–1736.
(18) Lo, K. K.-W.; Zhang, K. Y.; Leung, S.-K.; Tang, M.-C. *Angew. Chem., Int. Ed.* **2008**, *47*, 2213–2216.
(19) Ma, D.-L.; Wong, W.-L.; Chung, W.-H.; Chan, F.-Y.; So, P.-K.; Lai, T.-S.; Zhou, Z.-Y.; Leung, Y.-C.; Wong, K.-Y. *Angew. Chem., Int. Ed.* **2008**, *47*, 3735–3739.
(20) Sajoto, T.; Djurovich, P. I.; Tamayo, A. B.; Oxgaard, J.; Goddard, W. A., III; Thompson, M. E. *J. Am. Chem. Soc.* **2009**, *131*, 9813–9822.
(21) Sprouse, S.; King, K. A.; Spellane, P. J.; Watts, R. J. *J. Am. Chem. Soc.* **1984**, *106*, 6647–6653.
(22) Wilkinson, A. J.; Puschmann, H.; Howard, J. A. K.; Foster, C. E.; Williams, J. A. G. *Inorg. Chem.* **2006**, *45*, 8685–8699.
(23) Sun, Y. H.; Zhu, X.-H.; Chen, Z.; Zhang, Y.; Cao, Y. *J. Org. Chem.* **2006**, *71*, 6281–6284.
(24) Grosshenny, V.; Romero, F. M.; Ziessel, R. *J. Org. Chem.* **1997**, *62*, 1491–1500.
(25) (a) Rousseau, T.; Cravino, A.; Roncali, J.; Bura, T.; Ulrich, G.; Ziessel, R. *Chem. Commun.* **2009**, 1673–1675. (b) Rousseau, T.; Cravino, A.; Roncali, J.; Bura, T.; Ulrich, G.; Ziessel, R. *J. Mater. Chem.* **2009**, *19*, 2298–2300.

Complex 4. The complex **2** (0.050 g, 0.0605 mmol) was dissolved in acetonitrile (3 mL), and the Bodipy **3** (0.042 g, 0.0658 mmol) dissolved in benzene (10 mL) and triethylamine (3 mL) was dropwise added. The mixture vigorously degassed under argon and $[Pd(PPh_3)_4]$ (10 mg) was added as a solid. The mixture was heated at 60 °C during the night. The solution was cooled down to RT, and the solvent evaporated to dryness. The residue was dissolved in DMF (1 mL) and dropwise added through a pad of Celite into an aqueous solution of KPF_6 (0.500 g in 15 mL water). The precipitate was collected on paper and washed with water (3 times 100 mL). The complex was dried in air and was purified by column chromatography on alumina. The desired complex (red band) was eluted with a gradient of methanol (0−1%) in dichloromethane as mobile phase. The analytically pure complex was obtained as a red powder by crystallization in a mixture acetonitrile/diethylether (0.078 g, 96%). ^{1}H NMR (300.1 MHz, $CDCl_3$): δ 8.71 (m, 2H), 8.68 (d, ^3J = 8.3 Hz, 1H), 8.23 (t, ^3J = 8.3 Hz, 1H), 8.02 (d, ^4J = 1.7 Hz, 1H), 7.94 (m, 3H), 7.81−7.67 (m, 4H), 7.58 (d, ^3J = 8.3 Hz, 3H), 7.51 (d, ^3J = 6.0 Hz, 1H), 7.41 (t, ^3J = 7.2 Hz, 1H), 7.31 (d, ^3J = 8.3 Hz, 2H), 7.06 (m, 4H), 6.93 (q, ^3J = 7.2 Hz, 2H), 6.31 (d, ^3J = 7.5 Hz, 1H), 6.26 (d, ^3J = 7.5 Hz, 1H), 6.01 (s, 2H), 4.20 (s, 4H), 3.67−3.64 (m, 4H), 3.55−3.52 (m, 4H), 3.36 (s, 6H), 2.73 (s, 6H), 1.36 (s, 6H). $^{13}C\{^1H\}$ NMR (75.47 MHz, $CDCl_3$) δ 167.8, 167.7, 155.6, 155.2, 148.7, 143.5, 143.4, 140.7, 140.0, 138.2, 137.1, 132.6, 131.6, 130.9, 129.2, 128.7, 125.1, 124.9, 124.8, 123.5, 122.8, 121.9, 121.8, 119.7, 96.7, 92.8, 85.1, 71.8, 68.6, 59.6, 58.95, 16.1, 14.8 ppm. ESI-MS (positive mode in CH_3CN+CH_2Cl_2) m/z 1191.3 ($[M - PF_6]^+$. Anal. Calcd for $C_{65}H_{59}N_6O_4IrBPF_6$ (M_r = 1336.19): C, 58.43; H, 4.45; N, 6.29. Found C, 58.12, H, 4.24, N, 6.31.

Photophysical and Electrochemical Measurements. Static UV−vis absorption spectra were measured with a Hewlett-Packard 8453 diode array spectrophotometer or a Shimadzu UV-3600 dual-beam grating spectrophotometer. Steady-state photoluminescence spectra were obtained at room temperature and 77 K with a single photon counting spectrofluorimeter from Edinburgh Analytical Instruments (FL/FS 900) or on a HORIBA Jobin-Yvon fluoromax 4P spectrofluorimeter and corrected for detector response. The fluorescence quantum yield (Φ_{unk}) of **3** was calculated from eq 1 using rhodamine 6G in methanol (ϕ_{ref} = 0.78, λ_{exc} = 488 nm) as the reference. Here, F denotes the integral of the corrected fluorescence spectrum, A is the absorbance at the excitation wavelength, and n is the refractive index of the medium, *ref* and *unk* denote parameters from the reference and unknown experimental samples, respectively.

$$\Phi_{unk} = \Phi_{ref}\frac{F_{unk}A_{ref}n_{unk}^2}{F_{ref}A_{unk}n_{ref}^2} \quad (1)$$

The photoluminescence lifetime of **2** was measured using a nitrogen-pumped broadband dye laser (PTI GL-3300 N_2 laser, PTI GL-301 dye laser) as the excitation source. Pulse energies were typically attenuated to ~50 μJ/pulse, measured with a Molectron Joulemeter (J4−05). An average of 128 transients was collected, transferred to a computer, and processed using Origin 8.0. The fluorescence lifetime of **3** was measured on a PTI QuantaMaster spectrofluorimeter using TimeMaster software with Time-Correlated Single Photon Mode coupled to a Stroboscopic system. The excitation source was a thyratron-gated flash lamp filled with nitrogen gas. No filter was used for the excitation. An interference filter centered at 550 nm determined the emission monitoring bandpass. The instrument response function was determined by using a dilute colloidal silica light-scattering solution (LUDOX). Solutions prepared for photophysical experiments were optically dilute for steady-state photoluminescence (OD = 0.09−0.11) and for emission lifetime determination (OD = 0.01), whereas nanosecond transient absorption experiments utilized higher concentrations (OD = 0.2−0.8). In most instances, luminescence and nanosecond transient absorption samples in 1 cm path length anaerobic quartz cells (Starna Cells) were deoxygenated with solvent-saturated argon for at least 20 min prior to measurement.

Nanosecond transient absorption spectra were collected on a Proteus spectrometer (Ultrafast Systems) equipped with a 150 W Xe-arc lamp (Newport), a Bruker Optics monochromator (Chromex) equipped with two diffraction gratings blazed for visible and near-IR dispersion, respectively, and Si or InGaAs photodiode detectors (DET 10A and DET 10C, Thorlabs) optically coupled to the exit slit of the monochromator. Excitation at 450 nm with a power of 2.0 mJ/pulse from a computer-controlled Nd:YAG laser/OPO system from Opotek (Vibrant LD 355 II) operating at 10 Hz was directed to the sample with an optical absorbance of 0.4 at the excitation wavelength. The data consisting of a 128-shot average were analyzed by Origin 8.0 software.

Electrochemical measurements employed cyclic voltammetry with a conventional 3-electrode system using a BAS CV-50W voltammetric analyzer equipped with a Pt microdisk (2 mm^2) working electrode and a silver wire counter-electrode. Ferrocene was used as an internal standard and was calibrated against a saturated calomel reference electrode (SCE) separated from the electrolysis cell by a glass frit presoaked with electrolyte solution. Solutions contained the electro-active substrate in deoxygenated and anhydrous dichloromethane containing 0.1 M tetra-*n*-butylammonium hexafluorophosphate ($TBA^+PF_6^-$) as supporting electrolyte. The quoted half-wave potentials were reproducible within ≈ 10 mV.

Results and Discussion

Syntheses and Crystal Structure of 2. The pivotal starting material **2** was prepared in a single step from dimer **1** according to Scheme 1. The well-defined NMR spectra confirm that complex **2** is indeed a single isomer. Cross-coupling of **2** with the Bodipy dye **3** is made feasible by the use of Pd(0), and acetonitrile is required to solubilize the cationic Ir precursor. The dye is efficiently linked (96% yield) without decomposition of the iridium synthon. The well-defined ^{1}H NMR spectrum of the Ir/Bodipy hybrid (**4**) excludes the presence of aggregates and permits the conclusion that each moiety retains its own specificity without perturbing its neighbor, a situation also confirmed by the absorption, photophysical, and redox data (see below).

X-ray diffraction performed on a single crystal of **2** confirms the nature of the isomer and the presence of one hexafluorophosphate anion (PF_6^-) providing charge balance and two position-disordered acetonitrile molecules in the asymmetric unit. A perspective view of the cation is shown in Figure 1. The $[Ir(ppy)_2(bpy\text{-}CCH)]^+$ cation has a distorted octahedral coordination geometry with two ppy (ppy for 2-phenylpyridine) and one bpy-CCH (5-ethynyl-2,2′-bipyridine) around the iridium center, as indicated by the small bite angles of C23−Ir1−N3 [80.58(18)°], C34−Ir1−N4 [80.63 (19)°], and N2−Ir1−N1 [76.29 (16)°] and twisted bond angles of N3−Ir1−N4 [171.95(15)°], C34−Ir1−N2 [173.25(17)°], and C23−Ir1−N1 [173.00(17)°]. The coordination geometry of the ppy ligands around the cation is such that the nitrogen atoms N3 and N4 are in a *trans*- orientation, with Ir−N bond lengths of 2.047 (4) Å and 2.048 (4) Å, respectively; on the other hand, the metalated carbon atoms C23 and C34 of the ppy residues are

Scheme 1. Synthesis of Title Ir-Bodipy Chromophore[a]

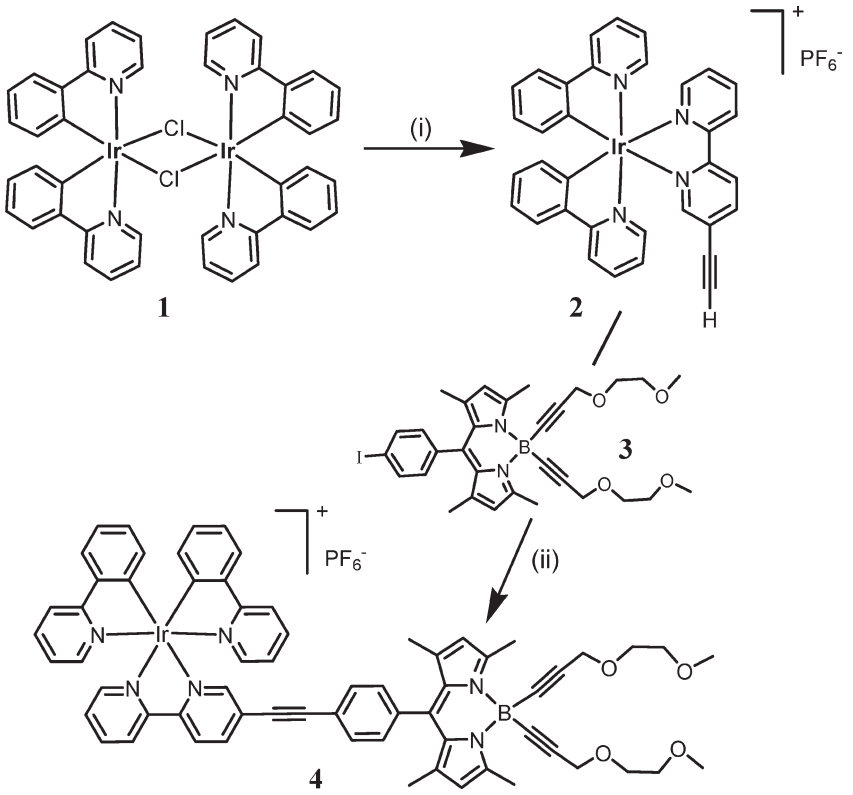

[a] Keys notes: (i) 5-ethynyl-2,2′-bipyridine (0.5 equiv), CH_2Cl_2/CH_3OH, 60°C, anion metathesis; (ii) [$Pd^0(PPh_3)_4$] (6 mol %), CH_3CN/benzene/triethylamine, 60°C.

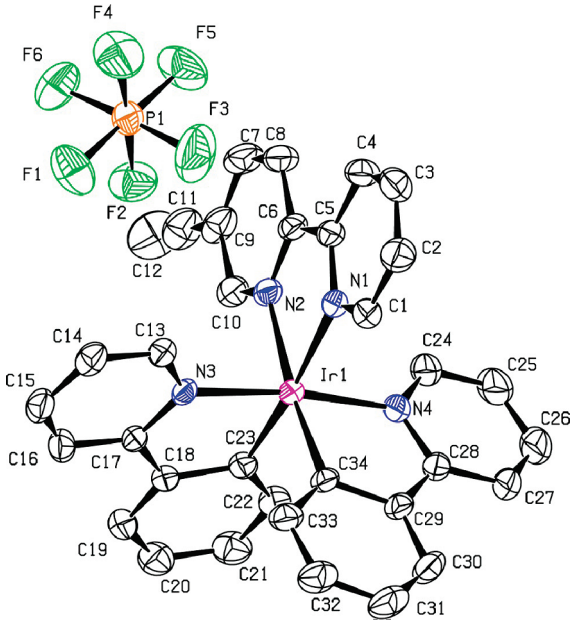

Figure 1. Perspective view of the [$Ir(ppy)_2$(bpy-CCH)](PF_6) **2** with atomic numbering scheme (ellipsoids at the 30% level). Acetonitrile solvent molecule and hydrogen atoms are omitted for clarity.

cis- positioned, with Ir−C bond lengths of 2.009 (5) Å and 2.018(5) Å, respectively. It should be noted that the Ir−N1 and Ir−N2 bond lengths in the bpy-CCH ligand are 2.145 (4) Å and 2.142 (4) Å, values, which are slightly longer than those in the ppy ligand. However, the bond lengths and angles are in agreement with related X-ray structures.[26]

In the crystal packing, the metal complex cations and PF_6^- anions are connected by weak C−H---F-P hydrogen bonds, mainly distributed along the [001] direction (see Supporting Information, Figure S1). The intra- and intermolecular C−H---F interactions involve C−H bonds from the ethynyl group (bond length being 2.44 Å and the bond angle 149.2°) or aromatic C−H bonds from pyridine rings of both bpy-CCH and ppy ligands. Three H---F distances are shorter than 2.5 Å with the shortest one of 2.33 Å ($\langle$C−H---*F*$\rangle$ = 164.9°) involving the C4 atom from bpy-CCH, confirming their significant role played in crystal cohesion.[27] Note that PF_6^- anions form a zigzag chain along the [010] direction through 3.175 Å long F3---F5 intermolecular contacts.

Electrochemistry. The electrochemical properties of **2**, **3**, and **4** were measured in dichloromethane, and the results are summarized in Table 1 presented in V versus SCE. Complex **2** exhibits a reversible one-electron oxidation at 1.29 V assigned to the oxidation of Ir(III) to Ir(IV).[28] Compared to the previously reported [$Ir(ppy)_2$(bpy)]$^+$ the

(26) (a) Su, H.-C.; Chen, H.-F.; Fang, F.-C.; Liu, C.-C.; Wu, C.-C.; Wong, K.-T.; Liu, Y.-H.; Peng, S.-M. *J. Am. Chem. Soc.* **2008**, *130*, 3413–3419. (b) Neve, F.; La Deda, M.; Crispini, A.; Bellusci, A.; Puntoriero, F.; Campagna, S. *Organometallics* **2004**, *23*, 5856–5863. (c) Waern, J. B.; Desmarets, C.; Chamoreau, L.-M.; Amouri, H.; Barbieri, A.; Sabatini, C.; Ventura, B.; Barigelletti, F. *Inorg. Chem.* **2008**, *47*, 3340–3348.

(27) Grepioni, F.; Cojazzi, G.; Draper, S. M.; Scully, N.; Braga, D. *Organometallics* **1998**, *17*, 296–307.

(28) Kim, J. II; Shin, I.-S.; Kim, H.; Lee, J.-K. *J. Am. Chem. Soc.* **2005**, *127*, 1614–1615.

Table 1. Absorption, Luminescence, and Redox Data (V vs SCE) in Dichloromethane for the Ir/Bodipy Complex **4** along with the Individual Modules **2** and **3**

	λ_{abs}, nm (ε, M^{-1} cm^{-1})	λ_{em}, nm (Φ_{em}, τ)	E_{00} (eV)	$E_{1/2}$(ox)[a] (ΔE_p mV)	$E_{1/2}$(red)[a] (ΔE_p mV)	E A^+/A^*	E A^*/A^-
2	405 (5740) 377 (7660) 330 (21150) 289 (39100) 266 (49200)	629 (0.027, 243 ns)	2.33	+1.29 (80)	−1.24 (70) −1.85 (irrev.)	−1.04	+1.09
3	501 (83500) 469 (sh, 16300) 239 (31400)	510 (0.92, 4.3 ns)	2.54	+1.08 (60)	−1.34 (70)	−1.46	+1.20
4	501 (83600) 472 (sh, 20300) 349 (50200) 269 (67000)			+1.08 (70) +1.28 (80)	−1.21 (60) −1.32 (60)	−1.46(B)[b] −1.05(Ir)[b]	+1.12 (Ir)[b] +1.22 (B)[b]

[a] Potentials determined by cyclic voltammetry in anhydrous and deoxygenated CH_2Cl_2 solution, containing 0.1 M $TBAPF_6$, [electrochemical window from +1.6 to −2.2 V], at a solute concentration of ~1.0 mM, using a scan rate of 200 mV/s. Potentials were standardized versus ferrocene (Fc) as internal reference and converted to the SCE scale assuming that $E_{1/2}$ (Fc/Fc^+) = +0.38 V (ΔE_p = 60 mV) vs SCE. For reversible processes $E_{1/2} = (E_{pa} + E_{pc})/2$. Error in half-wave potentials is ± 10 mV. For irreversible processes the peak potentials (E_{pa}) are quoted. All reversible redox steps result from one-electron processes except otherwise quoted. [b] Calculated using E_{00} for compounds **2** and **3**.

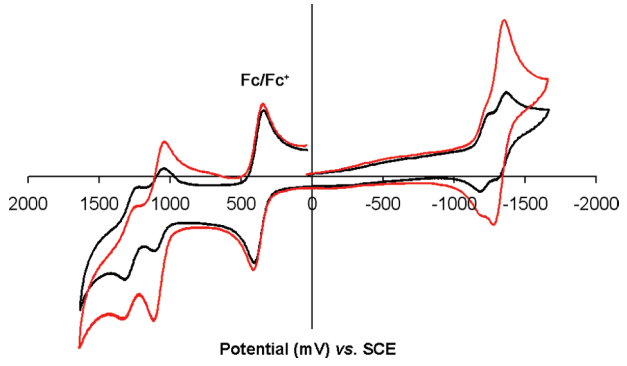

Figure 2. Cyclic voltammograms of complex **4** (black trace) and complex **4** with about 2 equiv of dye **3** (red trace), in dichloromethane at RT. The reversible Fc/Fc^+ redox couple at +0.38 V corresponds to genuine ferrocene.

oxidation of **2** is cathodically shifted by 140 mV because of the σ-withdrawing character of the ethynyl function compared to the unsubstituted bipyridine ligand.[29] One reversible reduction wave was found at −1.24 V safely assigned to the reduction of the ethynyl-bipyridine ligand. This reduction is also cathodically shifted by 270 mV compared to the $[Ir(ppy)_2(bpy)]^+$ complex; the destabilization of the lowest unoccupied molecular orbital (LUMO) is again due to the electron withdrawing effect of the ethynyl function compared to the bipyridine ligand leading to the conclusion that the bipyridine ligand is reduced before the phenylpyridine ligand.[28] Interestingly, a second irreversible reduction was observed at −1.85 V. In light of previous data, this process is assigned to the reduction of one of the orthometalated phenylpyridine ligands.[14]

The electrochemical data for **3** agrees with related Bodipy dyes and displays a reversible one-electron oxidation at 1.08 V due to radical cation formation and a reversible one-electron reduction at −1.34 V due to radical anion formation.[9,10,30] These redox couples provide an estimated HOMO−LUMO gap of 2.42 eV, in agreement with the fluorescence data from the singlet excited state (see below).[31] Both redox processes are highly reversible ($i_{pa}/i_{pc} \approx 1$), with a shape that is characteristic of Nernstian one-electron processes (ΔE_p = 60−70 mV).[32]

The cyclic voltammogram of **4** is provided in Figure 2 (see also Table 1). Remarkably, two well-resolved one-electron oxidations were observed at 1.28 and 1.08 V, similar to that of reference compounds **2** and **3**, respectively. In addition, two reversible one-electron reductions were found at −1.21 and −1.32 V, in good agreement with **2** and **3**. Clearly the first oxidation and the second reduction processes are assigned to the Bodipy moiety. Confirmation of this assignment was obtained by adding to the electrolytic solution of **4** the genuine Bodipy compound **3** (Figure 2 red trace). A significant enhancement of the first oxidation wave and the second reduction wave confirms that the Bodipy subunit is indeed responsible for these redox processes. Importantly, the electrochemical data suggest that the Ir and Bodipy moieties in **4** are electronically isolated from one another. The presence of the phenyl group in the meso position of the Bodipy is expected to be perpendicular due to the steric hindrance generated by the presence of both methyl groups in the 1- and 7- substitution positions. Many recent X-ray structures confirm this geometric arrangement which is sufficient to suppress extensive orbital overlap between both residues.[31]

Absorption and Emission Spectroscopy. The absorption spectra of all three chromophores along with the fluorescence of **3** are presented in Figure 3. The absorption of **2** is characterized by intense $\pi-\pi^*$ transitions from both ppy and bpy-CCH in the region of 250−330 nm. The ^{1}MLCT (metal-to-ligand charge-transfer) absorption has a λ_{max} = 377 nm (ε = 7660 M^{-1} cm^{-1}) whereas the direct singlet-to-triplet MLCT is located at λ_{max} = 468 nm (ε = 695 M^{-1} cm^{-1}), see also Supporting Information, Figure S2. This model chromophore exhibits an emission centered at 610 nm with a quantum yield of 0.027 measured relative to a $[Ru(bpy)_3]^{2+}$ quantum counter

(29) Slinker, J. D.; Gorodetsky, A. A.; Lowry, M. S.; Wang, J.; Parker, S.; Rohl, R.; Bernhard, S.; Malliars, G. G. *J. Am. Chem. Soc.* **2004**, *126*, 2763–2767.
(30) Goze, C.; Ulrich, G.; Ziessel, R. *J. Org. Chem.* **2007**, *72*, 313–322.
(31) Ziessel, R.; Ulrich, G.; Harriman, A.; Alamiry, M. A. H.; Stewart, B.; Retailleau, P. *Chem.—Eur. J.* **2009**, *15*, 1359–1369.
(32) Ziessel, R.; Bonardi, L.; Retailleau, P.; Ulrich, G. *J. Org. Chem.* **2006**, *71*, 3093–3102.

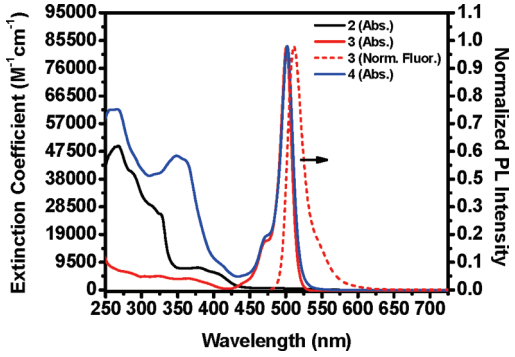

Figure 3. Absorption spectra of the three chromophores investigated in this study and the fluorescence of **3** measured in CH_2Cl_2 at RT.

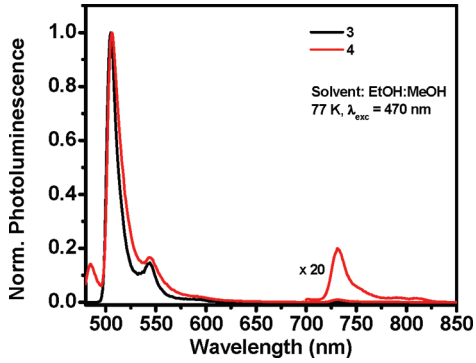

Figure 4. Normalized photoluminescence of **3** and **4** in a 77 K 4:1 EtOH/MeOH glass (λ_{ex} = 470 nm). The phosphorescence of **4** (λ_{em} = 733 nm) has been scaled by a factor of 20.

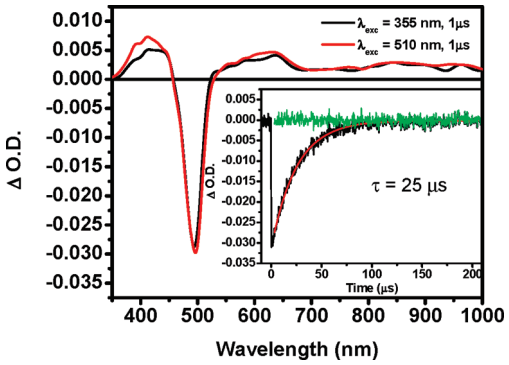

Figure 5. Transient absorption difference spectra of complex **3** in deaerated CH_2Cl_2 measured 1 μs after laser excitation (1.5 mJ/pulse) at 355 nm (black) or 510 nm (red). Inset: Single wavelength decay trace at 500 nm (black) along with the corresponding single-exponential fit (red) and residuals (green). All data were collected at 298 K.

(Supporting Information, Figure S3) and a lifetime of 243 ± 1 ns (Supporting Information, Figure S4). The low energy portion of the photoluminescence excitation spectrum completely superimposes the absorption spectrum of **2**. Reference compound **3** exhibits typical absorption transitions in the visible with the $S_0 \rightarrow S_1$ transition centered at 501 nm (ε = 83500 M^{-1} cm^{-1}) while the lower intensity $S_0 \rightarrow S_2$ transition is centered in the UV. The singlet fluorescence of **3** is observed at λ_{em} = 510 nm with a large quantum efficiency (Φ_{fl} = 0.92, τ_{fl} = 4.3 ns). Again, the excitation spectrum of **3** closely mimics that of the absorption profile. The absorption spectrum of **4** is mostly in agreement with a linear combination of model chromophores **2** and **3**. Key observations to note are that upon linkage of [Ir(ppy)$_2$(bpy-C≡C−)] to the Bodipy, the $S_0 \rightarrow S_1$ transition of the Bodipy moiety does not significantly shift in energy nor does the position of the ^{1}MLCT absorption. The most significant change in the absorption spectrum arises from a red-shift in a $\pi-\pi^*$ absorption of the bpy-C≡C- subunit. This absorption transition now significantly overlaps with the ^{1}MLCT absorption of the $Ir^{III}(ppy)_2$ moiety. Note that upon formation of the ethyne-bridge between the two chromophores, the phosphorescence observed in **2** is quantitatively quenched and the fluorescence intensity of **3** has been drastically reduced, irrespective of the excitation wavelength. This indicates that triplet energy transfer from Ir-based ^{3}CT excited state to the Bodipy subunit is facile in **4**, and the ^{1}Bodipy excited state is efficiently quenched in **4**. It is important to note that the complete lack of spectral overlap between the ^{1}Bodipy fluorescence and the ^{1}CT absorption precludes resonance energy transfer being responsible for the fluorescence quenching observed in **4**. The data presented below will suggest that intersystem crossing (facilitated by the Ir(III) center) to the ^{3}Bodipy excited state is responsible for the attenuation of the singlet fluorescence in **4** in relation to that measured in **3**.

Although no RT phosphorescence from ^{3}Bodipy was observed, cooling a 4:1 EtOH/MeOH solution of **4** to 77 K clearly reveals the presence of phosphorescence centered at 730 nm (Figure 4). Importantly, this excitation profile agrees quantitatively with the corresponding ground-state absorption spectrum. This emission profile agrees well with previous investigations which have demonstrated the sensitization of ^{3}Bodipy phosphorescence,[9,10] and establishes the Bodipy triplet state energy in this molecule. Thus, the lowest energy excited state in **4** is assigned as ^{3}Bodipy. This assignment is consistent with our findings from RT transient absorption measurements which are discussed below. Low temperature emission measurements performed on **3** clearly demonstrates that phosphorescence is not observed. However, identical long-wavelength Bodipy-based phosphorescence can be observed upon addition of 10% iodoethane, taking advantage of the external heavy atom effect. This induced phosphorescence needed to be magnified by a factor of 400 to be placed on the same intensity scale as that observed in complex **4** (Supporting Information, Figure S5). These low temperature photoluminescence experiments clearly demonstrate that the low energy emission in **4** indeed emanates from the triplet state of the Bodipy chromophoric subunit.

Transient Absorption Spectroscopy. We sought to further investigate the excited state dynamics of **4** using laser flash photolysis. The transient absorption difference spectra of **4** (Figure 5) were collected using two different excitation wavelengths. While 510 nm selectively excites the Bodipy moiety, we can also predominately excite the Ir(ppy)$_2$(bpy-C≡C−) moiety when using 355 nm laser excitation. In both cases, a lowest energy excited-state characterized as ^{3}Bodipy is formed. No kinetic information on the formation of the lowest energy excited state was obtained on the nanoseconds time scale where the impulse response function is approximately 10 ns. Both transient absorption difference spectra collected at 1 μs after the laser pulse exhibit a

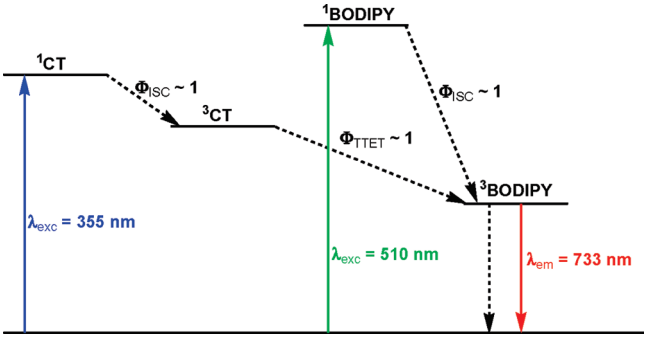

Figure 6. Proposed Jablonski diagram depicting relevant energy transfer pathways in **4**. Here ISC is intersystem crossing and TTET is triplet−triplet energy transfer. Dashed arrows indicate non-radiative transitions.

bleached signal centered at 500 nm which corresponds to the ground-state absorption profile of the Bodipy subunit, Figure 3. This ground state bleach recovers by single exponential kinetics that are adequately fit to an excited-state lifetime of 25 μs, much longer than nanosecond-based singlet excited-state dynamics measured in **3**. The excited-state absorptions centered near 400 and 530 nm to near-IR also decay with the same time constant of 25 μs. These transient difference features agree well with literature data on related structures which were assigned to $T_1 \rightarrow T_n$ transitions in the ^{3}Bodipy excited state.[9,10] Control experiments performed on **3** failed to produce any measurable transients in our experiments, $\tau < 10$ ns. Consistent with the singlet fluorescence data provided above, the triplet state of the Bodipy cannot be significantly populated in the absence of triplet sensitization or the presence of a heavy atom to facilitate direct intersystem crossing. Under exposure to 355 nm excitation, the former process likely dominates in **4** whereas 510 nm excitation relies solely on the internal heavy atom effect to produce the ^{3}Bodipy excited state. In both instances, the same difference spectrum is quantitatively produced demonstrating that either process leads to a long-lived (25 μs) pendant triplet excited state in the title compound useful for facilitating bimolecular chemistry.

Energy Level Diagram. The electrochemical and spectroscopic data may now be combined in an effort to better understand the resultant energy transfer processes occurring in the excited-state of **4** (Figure 6 and Table 1). Upon selective excitation of the Ir(III) moiety ($\lambda_{ex} = 355$ nm), efficient intersystem crossing rapidly produces the ^{3}CT excited state. The reduction potential of Bodipy is such that oxidative quenching of the ^{3}CT excited state would be an endothermic process. The driving force for reductive quenching is negligible as well. Hence, excited-state quenching of ^{3}[Ir(ppy)$_2$(bpy-C≡C−)]$^+$ exclusively follows a triplet−triplet energy transfer mechanism to ^{3}Bodipy as electron transfer is not energetically viable. When the Bodipy chromophore is selectively excited ($\lambda_{ex} = 510$ nm), oxidative quenching is possible with a driving force of 130 mV. However, no evidence for a radical anion is present in the transient absorption data. The relatively nonpolar nature of the CH_2Cl_2 solvent presumably cannot stabilize the charge-separated state. Another likely route for ^{1}Bodipy excited-state quenching is via efficient intersystem crossing provided by the Ir(III) center. Importantly, selective excitation of either chromophore in **4** produces precisely the same excited-state on long time scales as evidenced by transient absorption and low temperature photoluminescence. Therefore, depending upon excitation wavelength, efficient triplet−triplet energy transfer or intersystem crossing is observed for the title compound which ultimately produces a lowest energy long-lived excited-state assigned as ^{3}Bodipy.

Conclusions

In summary, we have synthesized and investigated the photophysical properties of a new Ir-Bodipy chromophore. Upon tethering the two independent moieties, certain observations are made. The photoluminescence observed in model compounds **2** and **3** (^{3}MLCT and ^{1}IL, respectively) are quantitatively quenched in **4** regardless of the excitation wavelength. Low temperature photoluminescence measurements confirm that the lowest excited state is best described as ^{3}Bodipy in nature. Transient absorption spectra measured at RT exhibit difference features attributable to a lowest energy long-lived excited-state as ^{3}Bodipy upon selective excitation of either moiety. These observations strongly suggest that an intramolecular triplet energy transfer occurs upon selective excitation of [Ir(ppy)$_2$(bpy-C≡C−)]$^+$ subunit to generate ^{3}Bodipy. On the other hand, selective excitation of Bodipy initially generates the ^{1}Bodipy excited state which then undergoes facile intersystem crossing to produce ^{3}Bodipy due to the large spin−orbit coupling afforded by the Ir^{III} center.

Acknowledgment. F.N.C. and A.A.R. acknowledge funding from the Air Force Office of Scientific Research (FA 9550-05-1-0276) and the National Science Foundation (CBET-0731153 and CHE-0719050). R.Z. and T.B. acknowledge the CNRS and the ECPM for partial financial support and Alexandre Haefele for helpful discussion. We also warmly thank Johnson Matthey PLC for a loan of iridium salts.

Supporting Information Available: Quantum yield and lifetime data, low temperature spectra as well as additional crystallographic information (crystal packing diagram and CIF file). This material is available free of charge via the Internet at http://pubs.acs.org.